Time-dependent electron kinetics in N_2 and H_2 for a wide range of the field frequency including electron-vibration superelastic collisions

J. Loureiro
Centro de Electrodinâmica da Universidade Técnica de Lisboa, Instituto Superior Técnico, 1096 Lisboa Codex, Portugal
(Received 30 June 1992)

Electron-energy distribution functions (EEDF), electron-transport parameters, and rate coefficients have been calculated by solving the time-dependent Boltzmann equation in weakly ionized plasmas in N_2 and H_2, for a wide range of the field frequency going from $\omega \ll \nu_e$ up to $\omega \gg \nu_m^e$, where ν_e and ν_m^e are two characteristic relaxation frequencies for energy and momentum transfer, respectively. The effects produced by the electron-vibration superelastic collisions have been taken into account in the Boltzmann equation and their influence in the electron transport has been analyzed in detail. Both the temporal behavior and the time-averaged value of the EEDF and of several macroscopic quantities have been obtained and discussed for different values of the field frequency. Among several other aspects, it is shown that the instantaneous power absorbed from the field and the one dissipated in electron collisions are not in phase, although, obviously, they exactly compensate each other on the average.

PACS number(s): 51.50.+v, 52.25.Dg

I. INTRODUCTION

In past years an increasing interest has been devoted to the theoretical and experimental characterization of radio-frequency (rf) discharges, owing to their wide applications in plasma surface technology, such as plasma deposition and plasma etching [1]. In this context, the knowledge of the time dependence of the electron-energy distribution function (EEDF) is especially important for the understanding of the properties of the collision-dominated bulk plasma in such discharges (see, e.g., the works of Winkler, Capitelli, and Makabe, and their coauthors, in Refs. [2,3]).

As extensively discussed in those previous publications [2,3], a qualitative analysis of the time dependence of the isotropic and of the directional components of the electron distribution function under the action of a rf electric field can be performed using two characteristic relaxation frequencies for energy and momentum transfer, ν_e and ν_m^e (with $\nu_e \ll \nu_m^e$), respectively, given by

$$\nu_e(u)=\frac{2m}{M}\nu_m(u)+\sum_j \nu_j(u)$$

and

$$\nu_m^e(u)=\nu_m(u)+\sum_j \nu_j(u) .$$

Here, $\nu_m(u)$ and $\nu_j(u)$ are the collision frequencies for elastic momentum transfer and for inelastic excitation of the jth state, respectively, m/M is the electron-molecule mass ratio, and u is the electron energy. In this analysis we can distinguish the following situations. (i) For low field frequencies $\omega \ll \nu_e$, the isotropic component (that is, the EEDF) follows in a quasistationary way the rf electric field, presenting consequently a very large time modulation in those parts of the relevant range of the electron energy where the above inequality is satisfied. Therefore, in this low-frequency limit, the EEDF can be obtained by solving the Boltzmann equation in a dc field for the different time-varying values of the rf field strength. (ii) When the field frequency increases up to $\nu_e \simeq \omega \ll \nu_m^e$, in most parts of the relevant electron-energy range, the time modulation of the EEDF is significantly reduced and a time-resolved solution of the Boltzmann equation is required instead of a quasistationary one. In this range of ω values the corresponding time-averaged value of the EEDF is only slightly dependent on the field frequency since the inequality $\omega \ll \nu_m^e$ holds in the whole significant electron-energy range. (iii) For higher values of ω, so that $\nu_e \ll \omega \simeq \nu_m^e$, the time modulation of the EEDF is strongly reduced. Moreover, if the frequency ν_m^e is independent of the electron energy, the EEDF can then be obtained by solving the Boltzmann equation in a dc field, with an effective field strength given by

$$E_{\text{eff}}=\frac{E_0}{\sqrt{2}}\frac{1}{[1+(\omega/\nu_m^e)^2]^{1/2}} ,$$

where $E_0/\sqrt{2}$ is the rms value of the harmonic electric field. That is the so-called "effective field approximation." Finally, we note that in this latter case the time-averaged value of the EEDF is strongly diminished as ω increases beyond the limit $\omega \simeq \nu_m^e$, excepting near the origin of the electron-energy space where the EEDF exhibits a strong peak.

The various situations described here have been analyzed in detail both for discharges in atomic and in molecular gases. Thus the EEDF has been obtained by using the quasistationary approximation [4] at low field frequencies $\omega \ll \nu_e$ and by using the effective field approximation, valid as $\nu_m^e(u)=$const, at the high-frequency limit [5] $\omega \gg \nu_e$. This latter case has also been extended to situations where ν_m^e is dependent on the elec-

tron energy by introducing an effective electric field [6] given by

$$E_e = \frac{E_0}{\sqrt{2}} \frac{1}{[1+(\omega/\nu_{ce})^2]^{1/2}} ,$$

where ν_{ce} is a momentum transfer collision frequency for the bulk electrons which can be somewhat arbitrarily chosen (see Ref. [6]). The intermediate range of the field frequency values, $\omega \simeq \nu_e$, has been treated by solving the time-dependent Boltzmann equation in the works of Winkler and Capitelli, and their coauthors [2,7], and more recently also in Ref. [8]. However, in all these works the field frequency has been considered smaller than ν_m^e, so that the anisotropic component of the electron distribution function follows instantaneously the rf electric field, whereas the time-averaged value of the EEDF remains practically unchanged as ω varies. Finally, the range of the field frequencies going from $\nu_e \simeq \omega \ll \nu_m^e$ up to $\nu_e \ll \omega \simeq \nu_m^e$ has been covered by Makabe and Goto [3] for molecular gases such as CH_4 and H_2. Nevertheless, in Ref. [3] the effects produced by the electron-vibration (e-V) superelastic collisions have not been taken into account in the Boltzmann equation.

It follows from the present discussion that we can expect an important time modulation of the EEDF for angular field frequencies such that $\omega \lesssim \nu_e$ in the whole significant electron-energy range. In an atomic gas discharge, at field frequencies not too low ($\omega \gtrsim 10^8$ s^{-1}) and at gas pressures typical of rf plasma processing, the inequality $\omega \lesssim \nu_e$ holds only in the high-electron-energy part of the EEDF, so that there is no modulation of the bulk electrons. We note that the characteristic frequency for energy transfer ν_e is a monotonously increasing function of the electron energy. Therefore the effective field approximation is a very satisfactory approach to describe these plasmas. However, this is no longer true if we deal with a molecular discharge, where the characteristic frequency ν_e presents significant values even at electron energies as low as a few eV (e.g., in N_2 at $u \simeq 2.5$ eV), as a result of the dissipation of electron energy in vibrational excitation. Obviously, in this latter case the effective field approximation cannot be used [7].

In this paper we present a theoretical approach based on the Boltzmann equation to the systematic investigation of the time dependence of the electron transport in a rf electric field bridging the whole range of the field frequency going from $\omega \ll \nu_e$ up to $\omega \gg \nu_m^e$. This study will be carried out for discharges in N_2 and H_2 both for the case of vanishingly small vibrational excitation $T_v \simeq T_g$, where T_v and T_g denote the vibrational and the gas temperatures, respectively, and for the case of appreciable vibrational excitation $T_v \gg T_g$. In the latter situation the e-V superelastic collisions are taken into account in the Boltzmann equation. Finally, we note that previous works having dealt with this subject have not considered the e-V superelastic collisions (in the case of Ref. [3]) or they have considered only the range of low field frequencies $\omega \ll \nu_m^e$, i.e., they have supposed the anisotropic component of the electron distribution in quasiequilibrium with the rf applied field (see, e.g., Ref. [7]).

II. THEORY

A. Basic theoretical formulation

In this section we summarize the present theoretical development of the spatially homogeneous Boltzmann equation under the influence of a time-varying sinusoidal electric field

$$\mathbf{E}(t) = \mathbf{E}_0 \cos(\omega t) , \tag{1}$$

with $\mathbf{E}_0 = -E_0 \mathbf{e}_z$, and where ω is the angular frequency.

The electron velocity distribution function $F(\mathbf{v},t)$ can be obtained by solving the time-dependent Boltzmann equation

$$\frac{\partial F}{\partial t} - \left[\frac{e}{m} \mathbf{E} \cdot \frac{\partial F}{\partial \mathbf{v}} \right] = I(F) + J(F) , \tag{2}$$

where e and m are the electron absolute charge and mass, respectively, $\mathbf{v}$ is the electron velocity, and I and J denote the collision operator for elastic and for inelastic collisions, respectively. In this paper we will neglect processes which result in the production or loss of electrons, i.e., attachment and production of secondary electrons by ionization, so that $J(F)$ includes only the effects of energy-exchange processes, both for inelastic and superelastic collisions. Therefore the electron velocity distribution is normalized through the condition

$$\int F(\mathbf{v},t) d^3 v = n_e , \tag{3}$$

where n_e denotes the time-independent electron number density.

Equation (2) is solved by expanding F in Legendre polynomials in velocity space and in Fourier series in time (see, e.g., Refs. [9,3]),

$$F(\mathbf{v},t) = \sum_{l=0} \sum_{k=0} \mathrm{Re}\{ \bar{F}_k^l(v) e^{jk\omega t} \} P_l(\cos\theta) , \tag{4}$$

where θ is the angle between $-\mathbf{E}_0$ and $\mathbf{v}$, $v = |\mathbf{v}|$, Re{ } means the "real part of," and $\bar{F}_k^l$ is a complex function expressing the time delay of the electron transport with respect to the applied electric field (1). Here, we will assume that the anisotropies resulting from the field are sufficiently small, so that the first two terms in spherical functions suffice for the expansion [10]

$$F(\mathbf{v},t) \simeq F^0(v,t) + F^1(v,t)\cos\theta . \tag{5}$$

Under this assumption, the lowest-order approximation for the expansion in Fourier series, allowing a periodic time variation in the isotropic velocity distribution (that is, in the EEDF), is given by

$$F^0(v,t) \simeq F_0^0(v) + F_2^0(v)\cos[2\omega t + \phi_2^0(v)] \tag{6}$$

and

$$F^1(v,t) \simeq F_1^1(v)\cos[\omega t + \phi_1^1(v)] . \tag{7}$$

As shown below, the fact that the isotropic and the anisotropic components of the electron distribution are functions of $E(t)^2$ and $E(t)$, respectively, originates that the isotropic velocity distribution, $F^0(v,t)$, only has even har-

monics in the Fourier expansion, whereas $F^1(v,t)$ only has odd ones. The normalization condition (3) appropriate to the present simplifications can be written as

$$\int_0^\infty F_0^0(v)4\pi v^2 dv = n_e \ , \tag{8}$$

$$\int_0^\infty F_{2R}^0(v)4\pi v^2 dv = 0 \ , \tag{9a}$$

and

$$\int_0^\infty F_{2I}^0(v)4\pi v^2 dv = 0 \ , \tag{9b}$$

where F_{2R}^0 and F_{2I}^0 denote, respectively, the real and the imaginary part of the complex function $\bar{F}_2^0 = F_2^0 \exp(j\phi_2^0)$.

Introducing (4) into Eq. (2), one obtains the following system of nonlocal equations in velocity space for F_0^0, $\bar{F}_2^0$, and $\bar{F}_1^1$, respectively:

$$\frac{1}{3v^2}\frac{d}{dv}\left[\frac{eE_0}{2m}v^2 \mathrm{Re}\{\bar{F}_1^1\}\right] = I_0(F_0^0) + J_0(F_0^0) \ , \tag{10}$$

$$j2\omega\bar{F}_2^0 + \frac{1}{3v^2}\frac{d}{dv}\left[\frac{eE_0}{2m}v^2\bar{F}_1^1\right] = I_0(\bar{F}_2^0) + J_0(\bar{F}_2^0) \ , \tag{11}$$

$$j\omega\bar{F}_1^1 + \frac{eE_0}{m}\frac{dF_0^0}{dv} + \frac{eE_0}{2m}\frac{d\bar{F}_2^0}{dv} = I_1(\bar{F}_1^1) + J_1(\bar{F}_1^1) \ . \tag{12}$$

In the absence of superelastic collisions and in the case of excitation only from the ground state (the inclusion of superelastic collisions and of excitation from states other than the ground state will be considered in Sec. II B), the collision terms are given by

$$I_0(F_0^0) = \frac{1}{v^2}\frac{d}{dv}\left[\frac{m}{M}\nu_m v^3\left[F_0^0 + \frac{kT_g}{mv}\frac{dF_0^0}{dv}\right]\right] \ , \tag{13}$$

$$J_0(F_0^0) = -\left[\sum_j \nu_j(v)\right]F_0^0(v) + \sum_j\left[\left[\frac{v+v_j}{v}\right]\nu_j(v+v_j)F_0^0(v+v_j)\right] \ , \tag{14}$$

$I_0(\bar{F}_2^0)$ is identical to the right-hand side of Eq. (13) but with $\bar{F}_2^0$, $J_0(\bar{F}_2^0)$ is identical to the right-hand side of Eq. (14) but with $\bar{F}_2^0$, and

$$I_1(\bar{F}_1^1) + J_1(\bar{F}_1^1) = -\nu_m^e \bar{F}_1^1 \ , \tag{15}$$

with

$$\nu_m^e = \nu_m + \sum_j \nu_j \ . \tag{16}$$

Here, M is the molecular mass, T_g is the gas temperature, k is the Boltzmann constant, ν_m is the frequency for momentum transfer in elastic collisions between electrons and neutrals, $\nu_j = N v \sigma_j$ is the frequency for inelastic excitation of the jth state, σ_j denotes the corresponding electron cross section, N is the gas number density, and $(v+v_j)$ is linked to the electron energy u and the energy threshold u_j through the expression $(v+v_j) = [2(u+u_j)/m]^{1/2}$. Finally, ν_m^e denotes an effective frequency for momentum transfer including both elastic and inelastic contributions [10]. As discussed in Ref. [10], the use of an effective frequency in Eq. (15) is justifiable in gases for which inelastic scattering is not negligible but is nearly isotropic. The evaluation of such an approximation in N_2 is treated in Ref. [11].

Substituting (15) into Eq. (12), one obtains for $\bar{F}_1^1$

$$\bar{F}_1^1 = -\frac{eE_0}{m(\nu_m^e + j\omega)}\frac{dF_0^0}{dv} - \frac{eE_0}{2m(\nu_m^e + j\omega)}\frac{d\bar{F}_2^0}{dv} \ . \tag{17}$$

This expression when inserted in Eqs. (10) and (11) allows us to write the following system of equations for F_0^0, F_{2R}^0, and F_{2I}^0:

$$-\frac{1}{6v^2}\left[\frac{eE_0}{m}\right]^2\frac{d}{dv}\left[v^2\left[A\frac{dF_0^0}{dv} + \frac{A}{2}\frac{dF_{2R}^0}{dv} + \frac{B}{2}\frac{dF_{2I}^0}{dv}\right]\right] = I_0(F_0^0) + J_0(F_0^0) \ , \tag{18}$$

$$-2\omega F_{2I}^0 - \frac{1}{6v^2}\left[\frac{eE_0}{m}\right]^2\frac{d}{dv}\left[v^2\left[A\frac{dF_0^0}{dv} + \frac{A}{2}\frac{dF_{2R}^0}{dv} + \frac{B}{2}\frac{dF_{2I}^0}{dv}\right]\right] = I_0(F_{2R}^0) + J_0(F_{2R}^0) \ , \tag{19a}$$

$$2\omega F_{2R}^0 + \frac{1}{6v^2}\left[\frac{eE_0}{m}\right]^2\frac{d}{dv}\left[v^2\left[B\frac{dF_0^0}{dv} + \frac{B}{2}\frac{dF_{2R}^0}{dv} - \frac{A}{2}\frac{dF_{2I}^0}{dv}\right]\right] = I_0(F_{2I}^0) + J_0(F_{2I}^0) \ , \tag{19b}$$

with

$$A = \frac{\nu_m^e}{\nu_m^{e2} + \omega^2} \tag{20a}$$

and

$$B = \frac{\omega}{\nu_m^{e2} + \omega^2} \ . \tag{20b}$$

Following a procedure first proposed by Allis [12], we will transform the system (18), (19) into another one written in terms of a sum of electron fluxes in energy space. So, at this point, we multiply both terms in each equation by $4\pi v^2$

and we renormalize the electron distribution function F^0 according to the condition $F^0(v,t)4\pi v^2 dv = n_e f^0(u,t)\sqrt{u}\, du$, with $u = \frac{1}{2}mv^2$, i.e., for $f_0^0(u)$ we have $\int_0^\infty f_0^0(u)\sqrt{u}\, du = 1$. With these modifications, and after division of all terms by $2n_e N\sqrt{u}$ in each equation, we readily obtain

$$-\frac{d}{du}\left\{\frac{u}{6\sigma_m^e}\left[\frac{eE_0}{N}\right]^2\frac{1}{1+(\omega/N)^2(m/2u\sigma_m^{e2})}\left[\frac{df_0^0}{du}+\frac{1}{2}\frac{df_{2R}^0}{du}+\frac{1}{2}\left[\frac{\omega}{N}\right]\sqrt{m/2u}\,\frac{1}{\sigma_m^e}\frac{df_{2I}^0}{du}\right]\right\}$$
$$=\frac{d}{du}\left[\frac{2m}{M}\sigma_m u^2\left[f_0^0+kT_g\frac{df_0^0}{du}\right]\right]-u\left[\sum_j \sigma_j(u)\right]f_0^0(u)+\sum_j\left[(u+u_j)\sigma_j(u+u_j)f_0^0(u+u_j)\right], \quad (21)$$

$$-\frac{\omega}{N}\sqrt{2mu}\,f_{2I}^0-\frac{d}{du}\left\{\frac{u}{6\sigma_m^e}\left[\frac{eE_0}{N}\right]^2\frac{1}{1+(\omega/N)^2(m/2u\sigma_m^{e2})}\left[\frac{df_0^0}{du}+\frac{1}{2}\frac{df_{2R}^0}{du}+\frac{1}{2}\left[\frac{\omega}{N}\right]\sqrt{m/2u}\,\frac{1}{\sigma_m^e}\frac{df_{2I}^0}{du}\right]\right\}=\mathcal{R}_1, \quad (22a)$$

where $\mathcal{R}_1$ is the right-hand side of Eq. (21) with f_{2R}^0, and

$$\frac{\omega}{N}\sqrt{2mu}\,f_{2R}^0+\frac{d}{du}\left\{\frac{u}{6\sigma_m^e}\left[\frac{eE_0}{N}\right]^2\frac{1}{1+(\omega/N)^2(m/2u\sigma_m^{e2})}\left[\left[\frac{\omega}{N}\right]\sqrt{m/2u}\,\frac{1}{\sigma_m^e}\left[\frac{df_0^0}{du}+\frac{1}{2}\frac{df_{2R}^0}{du}\right]-\frac{1}{2}\frac{df_{2I}^0}{du}\right]\right\}=\mathcal{R}_2, \quad (22b)$$

where $\mathcal{R}_2$ is the right-hand side of Eq. (21) with f_{2I}^0. In the rewriting of Eqs. (21) and (22) σ_m^e represents an effective electron cross section for momentum transfer given by $\sigma_m^e = \nu_m^e/(N\sqrt{2u/m})$.

The approach employed for solving these equations consisted in converting them into three coupled sets of K algebraic equations by finite differencing the electron-energy axis into K cells as described in Ref. [13]. These sets of algebraic equations were simultaneously solved by matrix inversion. The accuracy in the energy-averaged electron power balance achieved with the numerical solutions was always better than 10^{-6} for the three functions.

Once the functions $f_0^0(u)$, $f_{2R}^0(u)$, and $f_{2I}^0(u)$ are obtained, the anisotropic component $\bar{f}_1^1(u)$ is then calculated from Eq. (17) after the renormalization $\bar{F}_1^1(v)4\pi v^2 dv = n_e \bar{f}_1^1(u)\sqrt{u}\, du$. The drift velocity $\mathbf{v}_d(t) = v_d(t)\mathbf{e}_z$, the energy-averaged electron energy $\langle u\rangle(t)$, or, for example, the electron rate coefficient $C_j(t)$ for excitation of the jth state can now be readily obtained: (i)

$$v_d(t) = \mathrm{Re}\{\bar{V}_{d0}e^{j\omega t}\}, \quad (23)$$

with $\bar{V}_{d0}$ given by

$$\bar{V}_{d0} = \tfrac{1}{3}\sqrt{2/m}\int_0^\infty u\bar{f}_1^1(u)du; \quad (24)$$

(ii)

$$\langle u\rangle(t) = \int_0^\infty u^{3/2}f^0(u,t)du, \quad (25)$$

which can be written in the form

$$\langle u\rangle(t) = \langle u\rangle_0 + \langle u\rangle_{2R}\cos(2\omega t) - \langle u\rangle_{2I}\sin(2\omega t), \quad (26)$$

with $\langle u\rangle_0$ given by

$$\langle u\rangle_0 = \int_0^\infty u^{3/2}f_0^0(u)du, \quad (27)$$

and $\langle u\rangle_{2R}$ and $\langle u\rangle_{2I}$ given by similar expressions but with $f_{2R}^0(u)$ and $f_{2I}^0(u)$, respectively, in place of $f_0^0(u)$; and (iii)

$$C_j(t) = \langle v\sigma_j\rangle = \sqrt{2/m}\int_0^\infty u\sigma_j(u)f^0(u,t)du, \quad (28)$$

or in the form

$$C_j(t) = (C_j)_0 + (C_j)_{2R}\cos(2\omega t) - (C_j)_{2I}\sin(2\omega t), \quad (29)$$

with $(C_j)_0$ given by

$$(C_j)_0 = \sqrt{2/m}\int_0^\infty u\sigma_j(u)f_0^0(u)du, \quad (30)$$

and $(C_j)_{2R}$ and $(C_j)_{2I}$ given by similar expressions with $f_{2R}^0(u)$ and $f_{2I}^0(u)$.

The energy-averaged power balance is an excellent test to the accuracy of the numerical solutions. Thus we can obtain the energy-averaged power balance equation, per electron and at unit gas density, by multiplying Eqs. (21) and (22) by $u\sqrt{2/m}$ and then integrating over all energies. The resulting equations are

$$(P_E)_0 = (P_{\mathrm{el}})_0 + (P_{\mathrm{inel}})_0, \quad (31)$$

$$(P_E)_{2R} = (P_{\mathrm{el}})_{2R} + (P_{\mathrm{inel}})_{2R} + (P_\omega)_{2R}, \quad (32a)$$

and

$$(P_E)_{2I} = (P_{\mathrm{el}})_{2I} + (P_{\mathrm{inel}})_{2I} + (P_\omega)_{2I}, \quad (32b)$$

with each term given by

$$(P_E)_0 = \frac{eE_0}{2N}\mathrm{Re}\{\bar{V}_{d0}\}, \quad (33)$$

$$(P_E)_{2R} = (P_E)_0, \quad (34a)$$

$$(P_E)_{2I} = \frac{eE_0}{2N}\mathrm{Im}\{\bar{V}_{d0}\}, \quad (34b)$$

$$(P_{\rm el})_0=\frac{2m}{M}\sqrt{2/m}\int_0^\infty \sigma_m u^2\left[f_0^0+kT_g\frac{df_0^0}{du}\right]du\ , \quad (35)$$

$(P_{\rm el})_{2R}$ and $(P_{\rm el})_{2I}$ as in Eq. (35) but with f_{2R}^0 and f_{2I}^0,

$$(P_{\rm inel})_0=\sum_j u_j(C_j)_0\ , \quad (36)$$

$(P_{\rm inel})_{2R}$ and $(P_{\rm inel})_{2I}$ as in Eq. (36) but with $(C_j)_{2R}$ and $(C_j)_{2I}$,

$$(P_\omega)_{2R}=-\frac{2\omega}{N}\langle u\rangle_{2I}\ , \quad (37a)$$

and

$$(P_\omega)_{2I}=\frac{2\omega}{N}\langle u\rangle_{2R}\ . \quad (37b)$$

Finally, we note that following this formulation the instantaneous energy-averaged power absorbed from the field, per electron and at unit gas density, is given by

$$P_E(t)=\frac{(\mathbf{J}_e\cdot\mathbf{E})}{n_eN}=(P_E)_0[1+\cos(2\omega t)]-(P_E)_{2I}\sin(2\omega t)\ , \quad (38)$$

where $\mathbf{J}_e=-en_e\mathbf{v}_d$ denotes the electron current density.

B. Extension to molecular gases

In molecular gas discharges, such as, e.g., in N_2 or H_2, we need to include the excitation of rotational and vibrational levels in the collision term J of the Boltzmann equation.

The excitation of molecular rotations is taken into account through a continuous loss flux in energy space [14], which corresponds to including an additional term in the right-hand side of Eq. (21) given by

$$\frac{d}{du}(4B_0\sigma_0 u f_0^0) \quad (39)$$

and further similar terms in Eqs. (22) with f_{2R}^0 and f_{2I}^0. Here, B_0 is the rotational constant and $\sigma_0=8\pi q^2a_0^2/15$, where q is the electric quadrupole moment in units of ea_0^2 (= 1.01 in N_2 and = 0.62 in H_2), a_0 denoting the Bohr radius.

On the other hand, owing to the relatively large populations in the excited vibrational levels, $v>0$, of the electronic ground state $N_2(X\ ^1\Sigma_g^+)$ or $H_2(X\ ^1\Sigma_g^+)$ usually present in a discharge, the inelastic and superelastic collisions of the electrons with those molecules must be taken into account in Eqs. (21) and (22). Thus, in Eq. (21), for example, we must add the following terms:

$$\sum_{v,w}\delta_v[-u\sigma_{v,w}(u)f_0^0(u)+(u+u_{v,w})\sigma_{v,w}(u+u_{v,w})f_0^0(u+u_{v,w})]$$
$$+\sum_{w,v}\delta_w[-u\sigma_{w,v}(u)f_0^0(u)+(u-u_{v,w})\sigma_{w,v}(u-u_{v,w})f_0^0(u-u_{v,w})]\ , \quad (40)$$

whereas in Eqs. (22a) and (22b) we must include identical terms with f_{2R}^0 and f_{2I}^0, respectively. Here, $\delta_v=N_v/N$ represents the fractional population in the vth vibrational level, and $\sigma_{v,w}$ and $\sigma_{w,v}$ are the electron cross sections for the inelastic and superelastic e-V energy exchange $v\leftrightarrows w$, with $v<w$, respectively. In this paper the effects of e-V collisions have been included in the Boltzmann equation assuming modified Treanor vibrational distributions [15]. A self-consistent treatment of this problem should include the coupling between the EEDF, $f^0(u,t)$, and the vibrational distribution function (VDF) of molecules in the electronic ground state $N_2(X)$ or $H_2(X)$. This could be done by solving the Boltzmann equation and a system of rate balance equations for the vibrational levels including, besides the e-V processes, the vibration-vibration (V-V) and the vibration-translation (V-T) energy exchange processes. The coupling between the EEDF and the VDF has not been taken into account here in a fully self-consistent manner for the sake of clearness of the present paper. However, a complete description of this problem can be found in our previous publications [6,16,17], which treat the cases corresponding to a dc applied electric field [16,17] and to a high-frequency (hf) one with a frequency assumed sufficiently high so that the EEDF can be supposed as quasistationary [6].

Finally, we note that the characteristic relaxation frequencies ν_e and ν_m^e for energy and momentum transfer (referred to in Sec. I) must include the contributions due to the excitation of rotational and vibrational levels. Thus, even in the case of vanishingly small vibrational excitation, both frequencies must be corrected in order to include rotational first- and second-order collisions and vibrational first-order collisions, by writing [3]

$$\nu_e(u)=\frac{2m}{M}\nu_m(u)+8B_0\frac{d\nu_0(u)}{du}+\sum_v\nu_{0,v}(u)+\sum_j\nu_j(u) \quad (41)$$

and

$$\nu_m^e(u)=\nu_m(u)+2\nu_0(u)+\sum_v\nu_{0,v}(u)+\sum_j\nu_j(u)\ , \quad (42)$$

with $\nu_0(u)=N\sigma_0\sqrt{2u/m}$, and where we have assumed $\nu_{J,J+2}+\nu_{J,J-2}\simeq 2\nu_0$ and $(u_{J,J+2}-u_{J,J-2})/2=4B_0$, J denoting the quantum rotational number (see Refs. [14,18]). On the other hand, $\nu_{0,v}(u)$ is the collision frequency for the vibrational excitation $0\rightarrow v$. Figure 1 shows the ratios ν_e/N and ν_m^e/N, as a function of the electron energy, both for N_2 and H_2, in the case of absence of vibrational excitation, i.e., for $T_v=T_g$. We note that $\nu_e(u)/N$ presents a sharp maximum in N_2 at about

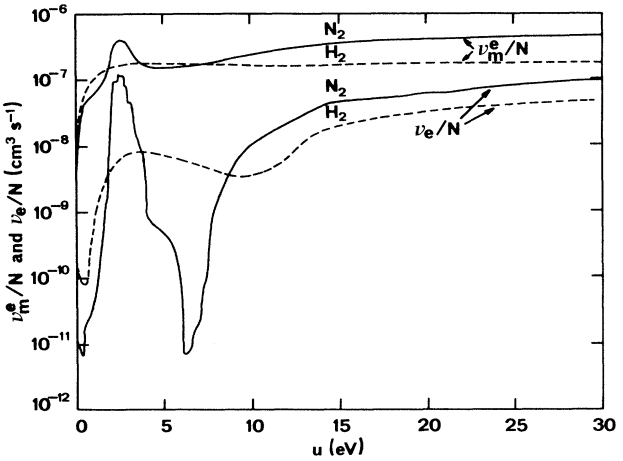

FIG. 1. Ratio of the characteristic relaxation frequency to the gas number density both for energy, ν_e/N, and momentum transfer, ν_m^e/N (see text). N_2—full curves; H_2—broken curves.

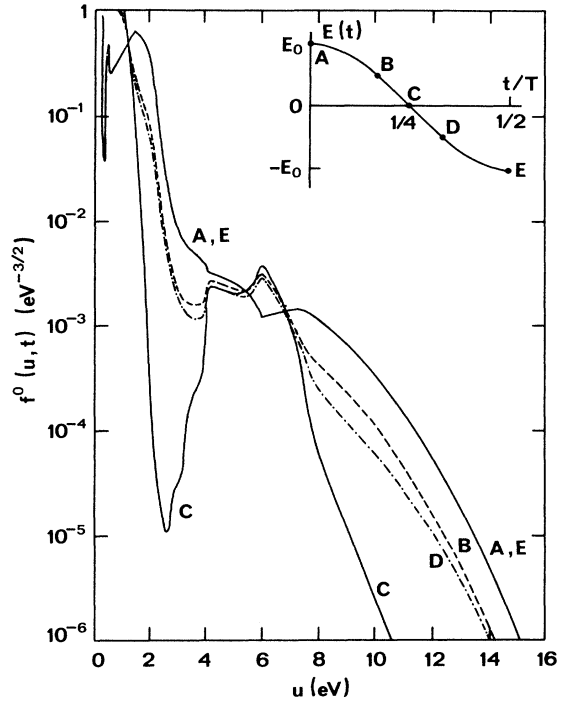

FIG. 2. EEDF in N_2 for $E_0/N=6\sqrt{2}\times10^{-16}$ V cm^2, $\omega/N=5\times10^{-10}$ cm^3 s^{-1}, and $T_v=T_g=400$ K. The various curves are for the following values of the reduced time t/T (T is the field period): 0 (A); $\frac{1}{6}$ (B); $\frac{1}{4}$ (C); $\frac{1}{3}$ (D); $\frac{1}{2}$ (E).

2.5 eV due to vibrational excitation and a monotonic growth at higher energies. On the contrary, in H_2 only a smooth maximum appears due to vibrational excitation.

III. RESULTS AND DISCUSSION

The Boltzmann equation, written in the form shown in Eqs. (21) and (22), can be solved to yield the EEDF, $f^0(u,t)$, as a function of the independent parameters: ratio of the electric field amplitude to the gas number density, E_0/N; ratio of the angular field frequency to the gas density, ω/N; gas temperature T_g; and vibrational temperature T_v. The latter parameter has been considered here in order to take into account the effects produced by the e-V superelastic collisions. The basic data on the electron cross sections used in this work are exactly the same as in Refs. [16,17] for N_2 and H_2, respectively, so that the reader should refer to those papers for details.

A. Discharges in N_2

Figure 2 shows the EEDF calculated in N_2 for $E_0/N=6\sqrt{2}\times10^{-16}$ V cm^2, $\omega/N=5\times10^{-10}$ cm^3 s^{-1}, and $T_v=T_g=400$ K, i.e., in the absence of appreciable vibrational excitation, and for the different times during half period of the rf electric field shown in the inset. For the considered rf field the EEDF oscillates with twice the field frequency presenting a modulation of many orders of magnitude and a small phase delay, relative to the applied electric field, in those parts of the electron-energy range where ω is appreciably smaller than the relaxation frequency for energy transfer, ν_e, plotted in Fig. 1. Thus the sharp maximum of ν_e/N at $u\simeq2.5$ eV, of about 10^{-7} cm^3 s^{-1}, due to vibrational excitation is clearly larger than the value chosen here for ω/N, so that for electron energies around 2.5 eV the EEDF follows the rf field in a quasistationary way excepting when the field goes through zero. We note that in this region of electron energies the EEDF is maximum when the absolute value of the rf field passes through its maximum, decreases strongly as the absolute value of the field decreases, and reaches a minimum when the field passes through zero. In particular, for zero field, the EEDF is extremely reduced and most of the electrons have only very small energy.

The other parts of the EEDF can be interpreted as well by looking at the dependence of the relaxation frequency ν_e on the electron energy shown in Fig. 1. There are two energy regions $u\lesssim1.5$ eV and $4\lesssim u\lesssim8$ eV practically devoid of vibrational or electronic inelastic processes, which correspond to relatively small values of ν_e/N. In both regions the inequality $\omega\ll\nu_e$ is no longer valid so the EEDF follows the rf field with a much smaller modulation and large phase delay. On the other hand, in the high-energy range $u\gtrsim8$ eV, dominated by the excitation of electronic states, the relaxation frequency ν_e has approximately the same magnitude as for $u\simeq2.5$ eV, so that the EEDF shows a very large modulation as well. Finally, it is interesting to note that, as a result of the nonequilibrium between the EEDF and the applied rf field, the EEDF is different at the instants t and $T/2-t$, T denoting here the field period. The EEDF is naturally larger when the rf field is decreasing, $0\le t\le T/4$, because of a memory effect. Obviously, the differences between the EEDF at both instants are decreasingly smaller as

ν_e/N increases, which is the case as the electron energy increases from $\simeq 8$ to $\simeq 14$ eV.

Figure 3 shows the various components of the EEDF, i.e., $f_0^0(u)$, $f_{2R}^0(u)$, and $f_{2I}^0(u)$, for the same conditions as in Fig. 2. In the electron-energy regions where $f^0(u,t)$ is strongly modulated f_{2R}^0 becomes close to f_0^0, which means that $f^0(u,t)$ oscillates between $\simeq 2f_0^0$ and nearly zero. On the other hand, the inequality $|f_{2I}^0| \ll f_{2R}^0$ indicates the existence of only a very small phase delay ϕ_2^0 in Eq. (6).

Figures 4(a)–4(d) show the EEDF calculated for $E_0/N = 6\sqrt{2}\times 10^{-16}$ V cm^2, $T_v = T_g = 400$ K, and the following increasing values of ω/N: 10^{-9}, 10^{-8}, 10^{-7}, and 10^{-6} cm^3 s^{-1}. For $\omega/N = 10^{-9}$ cm^3 s^{-1} we observe only a slight reduction of the magnitude of the time modulation of the EEDF with respect to Fig. 2, as in this case the field frequency is still largely smaller than ν_e in the electron-energy regions $1.5 \lesssim u \lesssim 4$ eV and $u \gtrsim 8$ eV. For $\omega/N = 10^{-8}$ cm^3 s^{-1} we have already $\omega \gtrsim \nu_e$ in large parts of the relevant range of the electron energies so that the modulation of the EEDF is strongly diminished. Finally, for $\omega/N = 10^{-7}$ cm^3 s^{-1} [Fig. 4(c)] we have no modulation since the inequality $\omega \gtrsim \nu_e$ holds in the entire electron-energy range. Furthermore, an increasing delay of $f^0(u,t)$ relative to the rf field occurs, approaching $T/4$, i.e., $\phi_2^0 \simeq -\pi$ in Eq. (6), as $\omega \to \infty$.

On the other hand, as long as ω is smaller than the relaxation frequency for momentum transfer ν_m^e, the time-averaged value of the EEDF, $f^0(u,t) = f_0^0(u)$, is only slightly dependent on ω, since, then, Eq. (21) becomes similar to the Boltzmann equation in a dc electric field of magnitude equal to the effective field strength $E_{\text{eff}} = E_0/\sqrt{2}$, excepting that in the present case we must keep in Eq. (21) the terms with f_{2R}^0 and f_{2I}^0 as well. The time-averaged value $f^0(u,t) = f_0^0(u)$ is strongly reduced when $\omega \gg \nu_m^e$, which is the case of Fig. 4(d) for $\omega/N = 10^{-6}$ cm^3 s^{-1}. As will be discussed below, when $\omega \gg \nu_m^e$ the time delay of the electron current density approaches $T/4$ and the electrons cannot gain energy from the electric field on the average. We note that when $\omega \gg \nu_m^e$ the time average over one period of Eq. (38) yields only a vanishingly small value $(\overline{\mathbf{J}_e \cdot \mathbf{E}}) \simeq 0$. Thus, for frequencies of this order, which correspond to microwave fields at gas pressures typical of plasma processing, the EEDF exhibits a strong peak at zero energy. This does not mean, of course, that a discharge cannot be sustained at such higher frequencies. For a given value of E_0/N kept constant, the effective electric field E_e (as defined in Sec. I) approaches zero when $\omega \to \infty$, so that the case plotted in Fig. 4(d) corresponds, in fact, to a vanishingly small value of E_e/N (see, e.g., Ref. [6] for the analysis of EEDF in this limiting case).

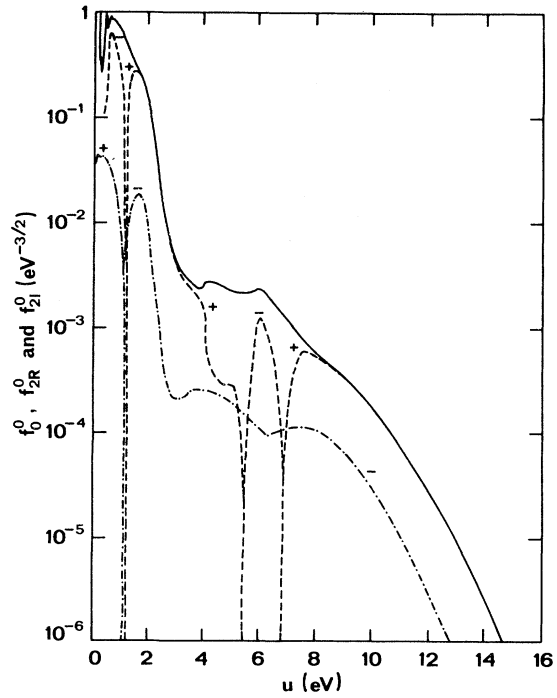

FIG. 3. Components of the EEDF in N_2 for the same conditions as in Fig. 2 (see text): f_0^0 (full curve); f_{2R}^0 (broken curve); f_{2I}^0 (chain curve).

The large modulation of the EEDF in the electron-energy range $1.5 \lesssim u \lesssim 4$ eV is strongly reduced when we consider the effects produced by the *e-V* superelastic collisions. Figure 5 shows the EEDF for the same values of E_0/N, ω/N, and T_g as in Fig. 2, but for the case of a vibrational excitation corresponding to a characteristic vibrational temperature $T_v = 4000$ K. The comparison between Figs. 2 and 5 allows us to evaluate the effects caused by the *e-V* superelastic collisions in reducing the effectiveness of the characteristic relaxation frequency for energy transfer ν_e, shown in Fig. 1, in the electron-energy range under discussion. The *e-V* superelastic collisions produce a decrease in the modulation amplitude and an increase in the phase delay of the EEDF, for energies $1.5 \lesssim u \lesssim 4$ eV, as well as an enhancement of the high-energy tail of the EEDF. This latter aspect has already been profusely discussed in previous papers [16,17]. It seems interesting at this point to compare the various components of the EEDF: $f_0^0(u)$, $f_{2R}^0(u)$, and $f_{2I}^0(u)$, calculated in the conditions of Fig. 2, and shown in Fig. 3, with those calculated in the conditions of Fig. 5 and now shown in Fig. 6. The *e-V* superelastic collisions produce an important reduction of f_{2R}^0 in the electron-energy range $1.5 \lesssim u \lesssim 4$ eV, which justifies the diminution of the time modulation previously discussed, and only have a small influence for the higher energies $u \gtrsim 8$ eV, where it remains $f_{2R}^0 \simeq f_0^0$. Finally, it is worth noting that the enhancement of the high-energy tail of the EEDF from Fig. 2 to Fig. 5 is not very significant because in these figures we have chosen a relatively high value of E_0/N. In the case of a lower value of E_0/N, e.g., as small as $3\sqrt{2}\times 10^{-16}$ V cm^2, the effects produced by the *e-V* superelastic collisions become much larger (see Ref. [16] for the analysis of this latter aspect).

Figure 7 shows the real and imaginary parts of the anisotropic complex function $\bar{f}_1^1(u)$, calculated for $E_0/N = 6\sqrt{2}\times 10^{-16}$ V cm^2, $T_v = T_g = 400$ K, and for $\omega/N = 5\times 10^{-10}$ cm^3 s^{-1}. For this relatively low value of ω/N, we have $\omega/N \ll \nu_m^e/N$ in the entire relevant

electron-energy range, so that the anisotropic component $f^1(u,t)$ follows the rf electric field with no delay. This can be observed in Fig. 7 due to the fact that the inequality $|f^1_{1I}| \ll f^1_{1R}$ practically holds in the entire electron-energy range, which means that there is no phase delay in $\bar{f}^1_1 = f^1_1 \exp(j\phi^1_1)$. On the contrary, when the equality $\omega/N \simeq \nu^e_m/N$ is approximately valid we have $|f^1_{1I}| \simeq f^1_{1R}$, with $f^1_{1R} > 0$ and $f^1_{1I} < 0$, which corresponds to a phase delay $\phi^1_1 \simeq -\pi/4$. Obviously, for larger values of ω/N, e.g., as high as 10^{-6} cm^3 s^{-1}, the imaginary part becomes

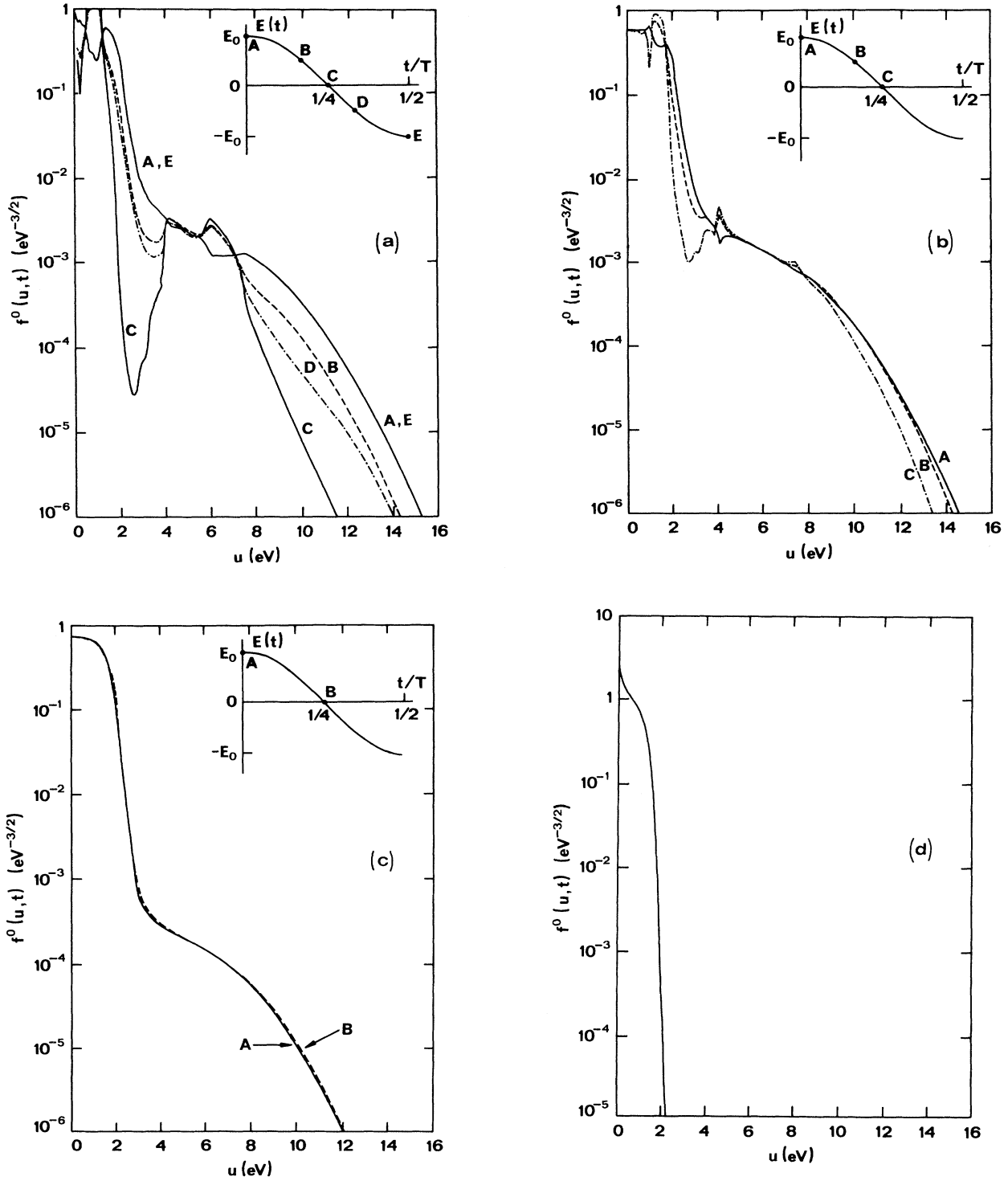

FIG. 4. EEDF in N_2 for $E_0/N = 6\sqrt{2}\times10^{-16}$ V cm^2, $T_v = T_g = 400$ K, and for the following values of ω/N in cm^3 s^{-1}: 10^{-9} (a); 10^{-8} (b); 10^{-7} (c); 10^{-6} (d). The various curves are for the instants shown in the inset.

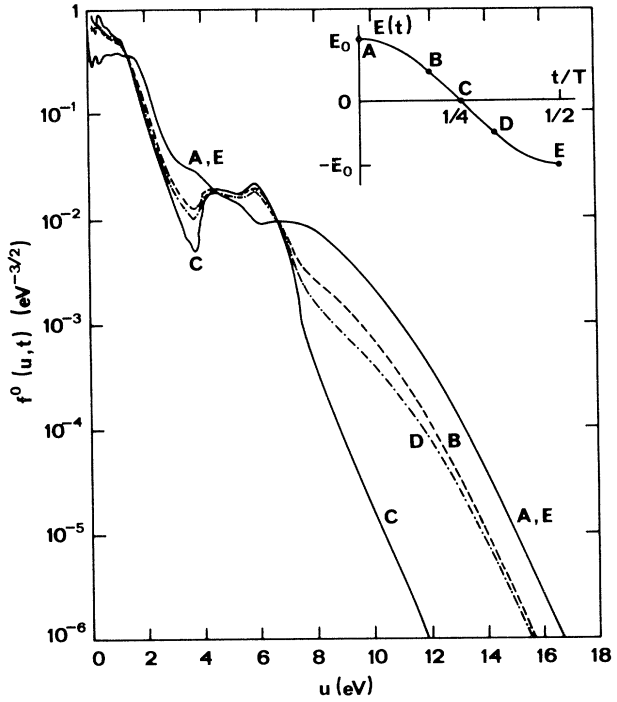

FIG. 5. As in Fig. 2 but for $T_v = 4000$ K.

predominant, $|f_{1I}^1| \gg f_{1R}^1$, and ϕ_1^1 approaches $-\pi/2$.

Keeping in mind the behavior of $f^1(u,t)$ as ω/N varies, the drift velocity, plotted in Fig. 8 as a function of time, can readily be interpreted. Figure 8 shows the drift velocity $[\mathbf{v}_d(t) = v_d(t)\mathbf{e}_z]$ calculated for the same values

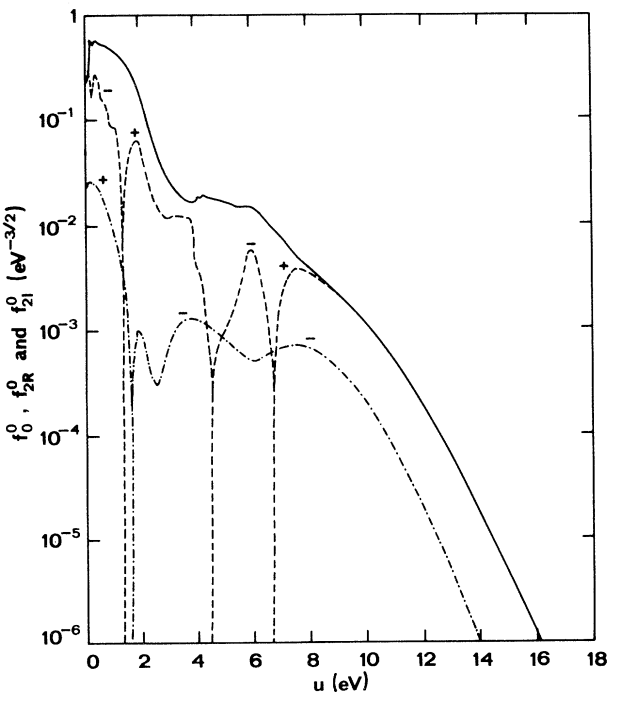

FIG. 6. As in Fig. 3 but for $T_v = 4000$ K.

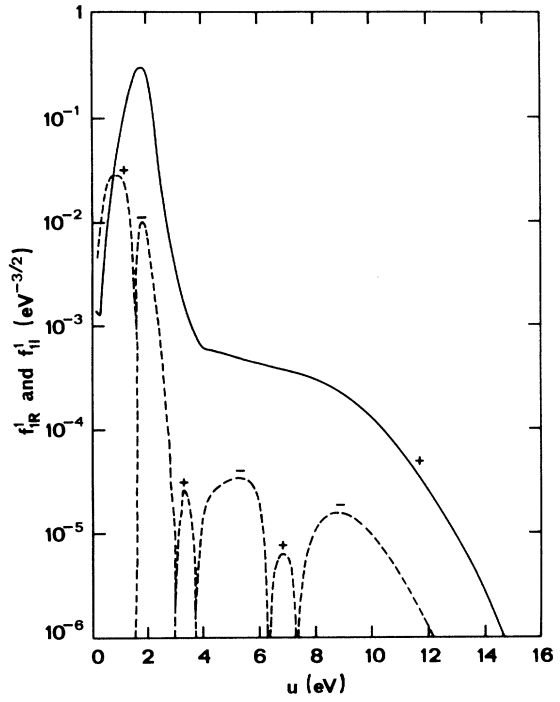

FIG. 7. Real and imaginary parts of the anisotropic complex function $\bar{f}_1^1$ in N_2 for $E_0/N = 6\sqrt{2}\times10^{-16}$ V cm^2, $T_v = T_g = 400$ K, and for $\omega/N = 5\times10^{-10}$ cm^3 s^{-1}. The full and broken curves are for f_{1R}^1 and f_{1I}^1, respectively.

of E_0/N and $T_v = T_g$ as in Fig. 7, and for various values of ω/N between 5×10^{-10} and 10^{-6} cm^3 s^{-1}. From inspection of Fig. 8 we can conclude that for $\omega/N \lesssim 10^{-8}$ cm^3 s^{-1} there is no delay relative to the applied field; for $\omega/N \simeq 10^{-7}$ cm^3 s^{-1} the phase delay is $\simeq -\pi/4$ in agreement with the fact that the equality $|f_{1I}^1| \simeq f_{1R}^1$ holds over most of the relevant electron-energy range; and for the highest values of ω/N the delay approaches $-\pi/2$. On the other hand, for the highest values of ω/N the drift velocity strongly reduces in magnitude.

For completeness, in Figs. 9 and 10 we present, respectively, the real part and the phase of the complex drift velocity $\bar{V}_{d0} = V_{d0}e^{j\Phi}$ as defined in Eq. (23). We note that

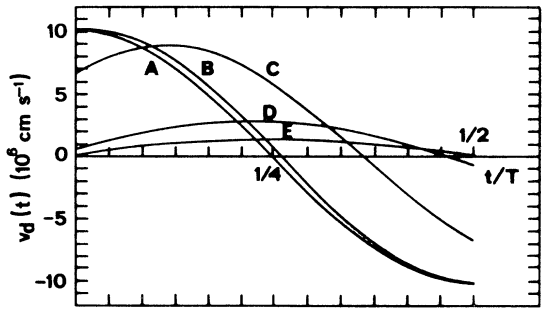

FIG. 8. Electron drift velocity in N_2 as a function of the reduced time t/T, for $E_0/N = 6\sqrt{2}\times10^{-16}$ V cm^2, $T_v = T_g = 400$ K, and for the following values of ω/N in cm^3 s^{-1}: 5×10^{-10} (A); 10^{-8} (B); 10^{-7} (C); 5×10^{-7} (D); 10^{-6} (E).

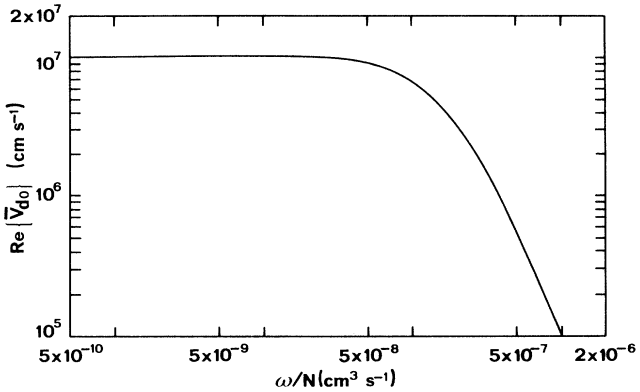

FIG. 9. Real part of the complex drift velocity in N_2 (see text) as a function of ω/N, for $E_0/N=6\sqrt{2}\times10^{-16}$ V cm^2 and $T_v=T_g=400$ K.

by writing $v_d(t)=V_{d0}\cos(\omega t+\Phi)$, the instantaneous energy-averaged power absorbed from the field, per electron and at unit gas density, given by Eq. (38), can be transformed in

$$P_E(t)=(P_E)_0+\frac{eE_0}{2N}V_{d0}\cos(2\omega t+\Phi)\ , \tag{43}$$

with $(P_E)_0$ given by Eq. (33). Thus Fig. 9 indicates that for $\omega/N\gtrsim10^{-7}$ cm^3 s^{-1} the real part of the drift velocity, $\mathrm{Re}\{\bar{V}_{d0}\}$, is significantly diminished, which corresponds to a reduction of the same magnitude in the time-averaged absorbed power $\overline{P_E(t)}=(P_E)_0$. In what concerns the instantaneous absorbed power, it oscillates with twice the field frequency and with the same phase delay Φ as the drift velocity plotted in Fig. 10.

Figures 11–13 show, as a function of the time, the energy-averaged electron energy, $\langle u\rangle(t)$, the electron rate coefficient for excitation of the first vibrational level $N_2(X\ ^1\Sigma_g^+,v=1)$, $C_{0,1}(t)$, and the electron rate coefficient for excitation of the entire electronic state $N_2(B\ ^3\pi_g)$, $C_X^B(t)$. These quantities have been calculated for $E_0/N=6\sqrt{2}\times10^{-16}$ V cm^2, $T_g=400$ K, various values of ω/N between 5×10^{-10} and 10^{-6} cm^3 s^{-1}, and for

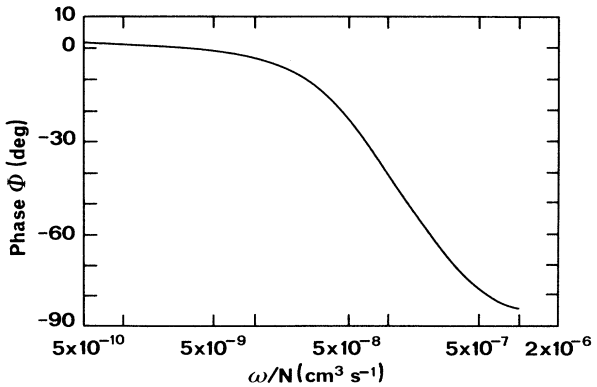

FIG. 10. Angular phase of the complex drift velocity in N_2, $\bar{V}_{d0}=V_{d0}\exp(j\Phi)$, for the same conditions as in Fig. 9.

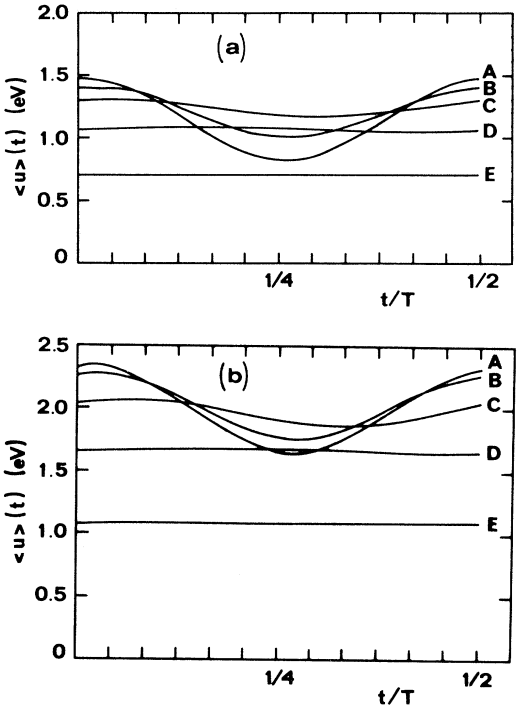

FIG. 11. Energy-averaged electron energy in N_2 as a function of the reduced time t/T, for $E_0/N=6\sqrt{2}\times10^{-16}$ V cm^2, $T_g=400$ K, and for $T_v=400$ K (a) and $T_v=4000$ K (b). The various curves are for the following values of ω/N in cm^3 s^{-1}: 5×10^{-10} (A); 10^{-9} (B); 10^{-8} (C); 10^{-7} (D); 10^{-6} (E).

$T_v=400$ K [in the case of Figs. 11(a), 12(a), and 13(a)] and $T_v=4000$ K (in the case of Figs. 11(b), 12(b), and 13(b)]. By inspection of these figures we can make the following remarks: there is a marked reduction in the time modulation (at the frequency 2ω) of all these quanti-

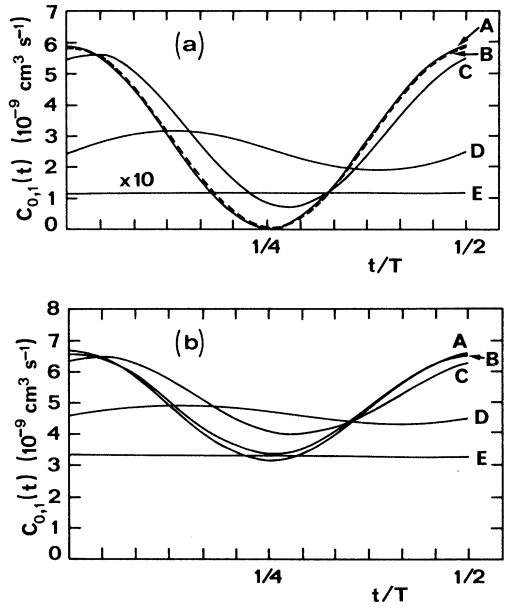

FIG. 12. Electron rate coefficient for vibrational excitation $N_2(X,v=0)\rightarrow N_2(X,v=1)$ in the same conditions as in Fig. 11.

ties as ω/N increases; there is an increasing phase delay which approaches $-\pi$, i.e., a time delay $\Delta t \simeq T/4$, as $\omega \to \infty$; the effects produced by the e-V superelastic collisions in reducing the time modulation are small for $\langle u \rangle(t)$ and $C_X^B(t)$, but they are extremely important for $C_{0,1}(t)$, which is a consequence of the behavior of the EEDF within the electron-energy range $1.5 \lesssim u \lesssim 4$ eV, as previously pointed out (see Figs. 2 and 5); the e-V superelastic collisions produce a general increase in all these quantities as T_v grows from 400 to 4000 K, and, in particular, they originate a strong increase in the electron rate coefficient $C_X^B(t)$. We note that this latter effect has already been discussed in detail in a previous paper [16] and is a consequence of the enhancement of the high-energy tail of the EEDF due to the e-V superelastic collisions. It is still worth noting at this point that as ω/N increases, the time delay of all these quantities approaches $\Delta t = T/4$, and not $T/8$ as stated in Ref. [2]. The value $T/8$ resulted from the fact that the authors of Ref. [2] imposed the condition $\omega \ll \nu_m^e$ in their papers.

Figures 14 and 15 show the time-averaged quantities $\overline{\langle u \rangle}$ and $\overline{C_{0,1}}$, respectively, as a function of ω/N, and for the same values of E_0/N, T_g, and T_v as in Figs. 11 and 12. The fall-off of all these functions as ω/N increases is a consequence of the decrease in the time-averaged value of the EEDF, $f^0(u,t) = f_0^0(u)$, as ω reaches its higher values ($\omega \gg \nu_m^e$).

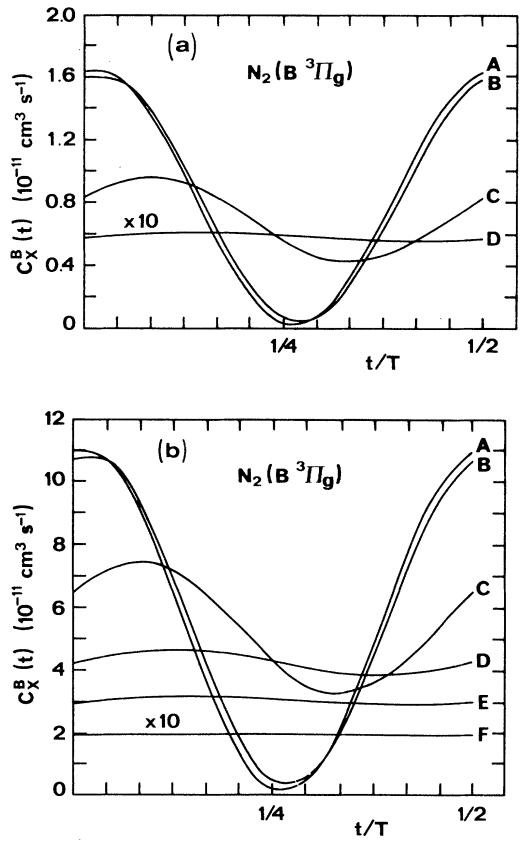

FIG. 13. Electron rate coefficient for excitation of the electronic state $N_2(B\ ^3\pi_g)$ as a function of the reduced time t/T, for $E_0/N = 6\sqrt{2} \times 10^{-16}$ V cm^2, $T_g = 400$ K, and for $T_v = 400$ K (a) and $T_v = 4000$ K (b). The various curves are for the following values of ω/N in cm^3 s^{-1}: (a) 5×10^{-10} (A); 10^{-9} (B); 10^{-8} (C); 10^{-7} (D); (b) 5×10^{-10} (A); 10^{-9} (B); 10^{-8} (C); 5×10^{-8} (D); 10^{-7} (E); 5×10^{-7} (F).

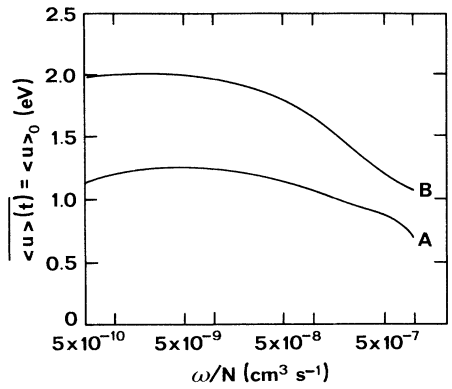

FIG. 14. Time-averaged mean electron energy, $\overline{\langle u \rangle(t)}$, in N_2 as a function of ω/N, for $E_0/N = 6\sqrt{2} \times 10^{-16}$ V cm^2, $T_g = 400$ K, and for $T_v = 400$ K (curve A) and $T_v = 4000$ K (curve B).

It follows from the present discussion that the instantaneous energy-averaged power absorbed from the rf field and the instantaneous power lost in electron collisions are not in phase with each other. More precisely, the time modulation of the instantaneous power lost by electron collisions is strongly diminished and its phase delay approaches $-\pi$ (i.e., $\Delta t = T/4$) as ω/N increases, whereas the instantaneous power absorbed from the field shows no reduction in modulation and has an increasing phase delay Φ going to $-\pi/2$ [i.e., $\Delta t = T/8$, see Eqs. (38) and (43)]. Obviously, the time-averaged values of both quantities exactly compensate each other and both go towards zero as ω/N increases beyond the limit $\omega/N \simeq \nu_m^e/N$. We note that $P_E(t) \simeq -(P_E)_{2I}\sin(2\omega t)$ as $\omega \to \infty$. Figures 16(a) and 16(b) show the instantaneous energy-

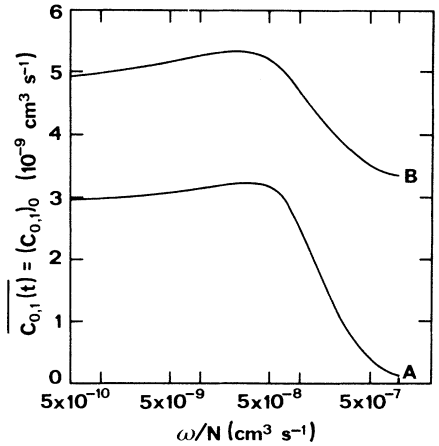

FIG. 15. Time-averaged electron rate coefficient for vibrational excitation $N_2(X,v=0) \to N_2(X,v=1)$, as a function of ω/N and for the same conditions as in Fig. 14.

averaged power absorbed from the field, $P_E(t)$, and that lost in electron collisions, $P_{\text{loss}}(t)$, per electron at unit gas density and as a function of time, for $E_0/N=6\sqrt{2}\times10^{-16}$ V cm^2, $T_v=T_g=400$ K, and for increasing values of ω/N going from 10^{-8} to 5×10^{-7} cm^3 s^{-1}. For the highest value of ω/N, $P_{\text{loss}}(t)$ is no longer modulated in time, while the phase delay of $P_E(t)$ clearly approaches $-\pi/2$.

B. Discharges in H_2

Figure 17 shows the EEDF in H_2 calculated for $E_0/N=3\sqrt{2}\times10^{-16}$ V cm^2, $\omega/N=2\times10^{-9}$ cm^3 s^{-1}, $T_v=T_g=400$ K, and for the different times shown in the inset. As seen from this figure, as compared with those presented before for N_2, the time modulation clearly is less pronounced here than in N_2, which is a consequence of the relative magnitudes of the relaxation frequency for energy transfer in both gases plotted in Fig. 1. The ratio of the relaxation frequency to the gas density, ν_e/N, is about one order of magnitude smaller in H_2 than in N_2 and, furthermore, in H_2 the ratio ν_e/N does not present any pronounced maximum due to the dissipation of electron energy in vibrational excitation as in N_2 at 2.5 eV. The absence of such a maximum in H_2 originates that in this case the effects of e-V superelastic collisions produce

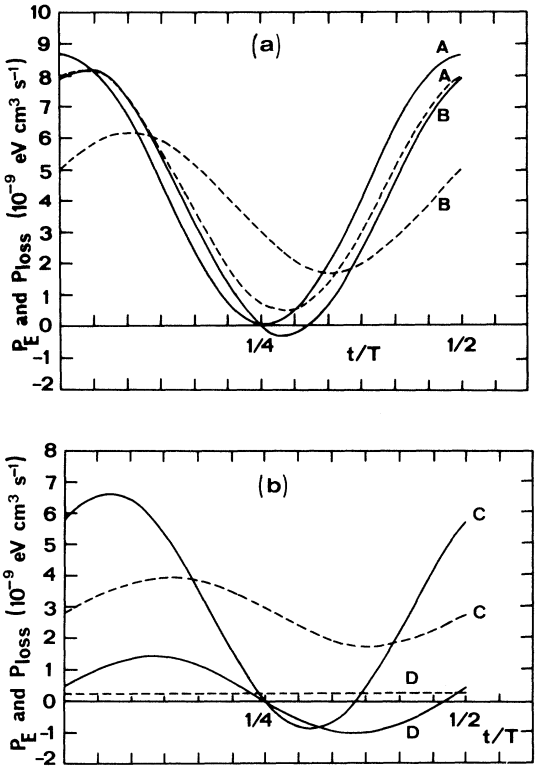

FIG. 16. Instantaneous energy-averaged power absorbed from the field (full curves) and the one lost in electron collisions (broken curves) in N_2, as a function of the reduced time t/T, for $E_0/N=6\sqrt{2}\times10^{-16}$ V cm^2, $T_v=T_g=400$ K, and for the following values of ω/N in cm^3 s^{-1}: (a) 10^{-8} (A); 5×10^{-8} (B); (b) 10^{-7} (C); 5×10^{-7} (D).

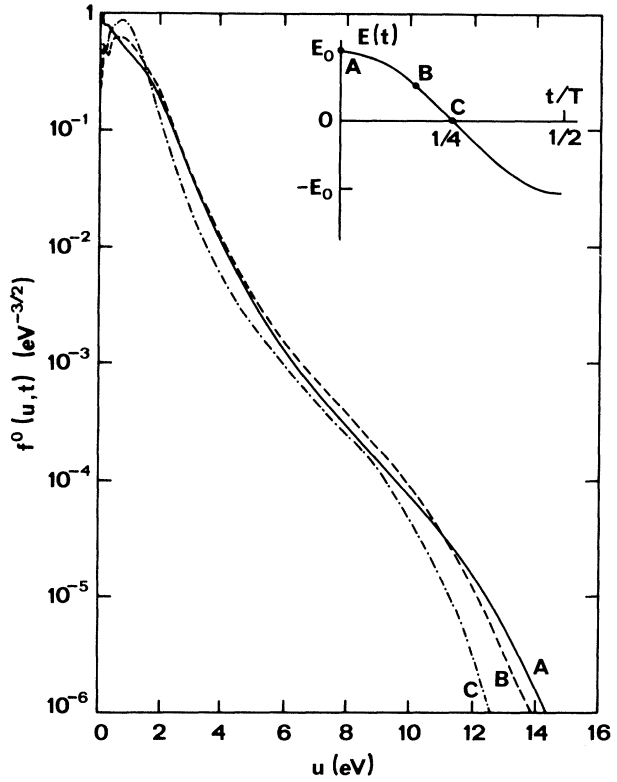

FIG. 17. EEDF in H_2 for $E_0/N=3\sqrt{2}\times10^{-16}$ V cm^2, $\omega/N=2\times10^{-9}$ cm^3 s^{-1}, $T_v=T_g=400$ K, and for the following instants t/T: 0 (A); $\frac{1}{6}$ (B); $\frac{1}{4}$ (C).

only minor modifications in the EEDF as compared to those observed in N_2.

Figure 18 shows the electron rate coefficient for the vibrational transition $H_2(X\,^1\Sigma_g^+,\ v=0)\rightarrow H_2(X\,^1\Sigma_g^+,\ v=1)$, plotted as a function of time, for $E_0/N=3\sqrt{2}\times10^{-16}$ V cm^2, $T_g=400$ K, $T_v=400$ K [Fig. 18(a)], and $T_v=3000$ K [Fig. 18(b)], and for the following values of ω/N: 2×10^{-9}; 10^{-8}; and 10^{-7} cm^3 s^{-1}. The basic trends presented in this figure are very similar to those shown before in Fig. 12 for N_2, but now the modifications due to the e-V superelastic collisions occur to a smaller extent. Finally, Table I presents further data on the electron rate coefficients for excitation of the triplet electronic state $H_2(b\,^3\Sigma_u^+)$, which dissociates to yield two H(1s) atoms, and for excitation of the singlet state $H_2(B\,^1\Sigma_u^+)$. Table I shows the time-averaged value of these coefficients, $\overline{C_j(t)}$, as well as the ratio of the 2ω component, $(C_j)_2$, to the time-averaged value, $\overline{C_j(t)}=(C_j)_0$. This ratio constitutes a measure of the degree of time modulation exhibited by each of these rate coefficients. It seems worth remembering here that Eq. (29) may be written as follows:

$$C_j(t)=(C_j)_0+(C_j)_2\cos(2\omega t+\varphi)\ . \tag{44}$$

The changes produced in both electronic rate coefficients as ω/N increases and T_v grows from 400 to 3000 K follow the same basic trends as in N_2, but now the effects

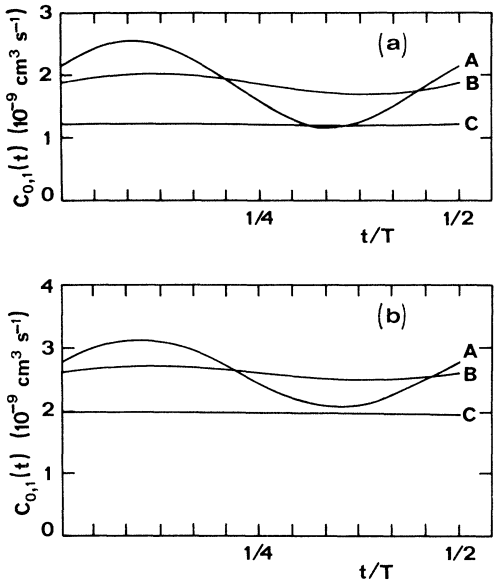

FIG. 18. Electron rate coefficient for vibrational excitation $H_2(X,v=0)\rightarrow H_2(X,v=1)$ as a function of the reduced time t/T, for $E_0/N=3\sqrt{2}\times10^{-16}$ V cm^2, $T_g=400$ K, and for $T_v=400$ K (a) and $T_v=3000$ K (b). The various curves are for the following values of ω/N in cm^3 s^{-1}: 2×10^{-9} (A); 10^{-8} (B); 10^{-7} (C).

produced by the e-V superelastic collisions are less pronounced.

IV. CONCLUSIONS

We have carried out a systematic investigation, based on the Boltzmann equation, of the time dependence of the electron transport in N_2 and H_2, under the action of a time-varying sinusoidal electric field. The present approach allows us to bridge the entire range of the field frequency going from $\omega\ll\nu_e$ up to $\omega\gg\nu_m^e$, where ν_e and ν_m^e, with $\nu_e\ll\nu_m^e$, denote two relaxation frequencies for energy and momentum transfer, respectively. The role played by the e-V superelastic collisions has been analyzed in detail.

The main conclusions of the present paper can be summarized as follows.

(i) EEDF, electron transport, and rate coefficients. For the low field frequencies $\omega\ll\nu_e$, the EEDF follows instantaneously the applied rf field showing a large time modulation of many orders of magnitude at twice the field frequency. As ω increases the EEDF presents a modulation and a delay relative to the applied field which become increasingly smaller and larger, respectively. In particular, when the inequality $\omega\gg\nu_e$ holds over most of the relevant electron-energy range, there is no modulation and the time delay increases up to $\frac{1}{4}$ of the field period. This limiting case corresponds therefore to the so-called effective field approximation. In the case of appreciable vibrational excitation, when $\omega\lesssim\nu_e$ the modulation of the EEDF is significantly reduced in a narrow electron-energy range ($1.5\lesssim u\lesssim4$ eV in N_2), as a result of a smaller effectiveness of the relaxation frequency ν_e, due to the effects produced by the e-V superelastic collisions. On the other hand, as long as the inequality $\omega\ll\nu_m^e$ is satisfied, the time-averaged value of the EEDF is only slightly dependent on ω. This is no longer true as ω increases beyond the limit $\omega\simeq\nu_m^e$ and, in particular, when the inequality $\omega\gg\nu_m^e$ holds in most of the electron-energy range the time-averaged value of the EEDF is dramatically diminished. Qualitatively, the electron-transport parameters and the electron rate coefficients for excitation and ionization exhibit similar features.

(ii) Anisotropic component of the electron distribution function, drift velocity, and power absorbed from the electric field. The directional component of the electron distribution function and the drift velocity follow instantaneously the applied field when the inequality $\omega\ll\nu_m^e$ is satisfied in the entire range of the electron energies. For higher values of ω both quantities show a strong reduction in their magnitudes and present an increasing time delay that approaches $\frac{1}{4}$ of the field period when $\omega\gg\nu_m^e$. It follows from this fact that the instantaneous energy-averaged power absorbed by the electrons from the field is a time-modulated function at 2ω, which is in quasiequilibrium with the field when $\omega\ll\nu_m^e$. However, for higher values of ω the instantaneous power absorbed from the field presents a strong reduction in its magnitude and an increasing time delay, which reaches $\frac{1}{8}$ of the field period in the limit $\omega\gg\nu_m^e$. We further note that the instantaneous absorbed power remains time modulated, even for the highest values of ω, while its time-averaged value decreases to zero. This latter aspect is a consequence of the time delay of the drift velocity approaching $\frac{1}{4}$ of the field period when $\omega\gg\nu_m^e$, and, therefore, of the fact that the electrons cannot gain energy from the field on the average in this limit. Finally, we note that the power absorbed from the field and that lost in electron

TABLE I. Time-averaged rate coefficient and ratio of the component in 2ω to the one independent of time, both for excitation of the entire electronic states $H_2(b\,^3\Sigma_u^+)$ and $H_2(B\,^1\Sigma_u^+)$, for $E_0/N=3\sqrt{2}\times10^{-16}$ V cm^2, $T_g=400$ K, $T_v=400$ and 3000 K, and for various values of ω/N.

ω/N (cm^3 s^{-1})	$H_2(b\,^3\Sigma_u^+)$				$H_2(B\,^1\Sigma_u^+)$			
	$\overline{C_X^b(t)}=(C_X^b)_0$ (10^{-12} cm^3 s^{-1})		$(C_X^b)_2/(C_X^b)_0$		$\overline{C_X^B(t)}=(C_X^B)_0$ (10^{-13} cm^3 s^{-1})		$(C_X^B)_2/(C_X^B)_0$	
	$T_v=400$ K	$T_v=3000$ K	$T_v=400$ K	$T_v=3000$ K	$T_v=400$ K	$T_v=3000$ K	$T_v=400$ K	$T_v=3000$ K
2×10^{-9}	0.616	3.147	0.768	0.716	0.344	1.811	0.974	0.958
10^{-8}	0.350	2.792	0.251	0.235	0.170	1.428	0.504	0.486
10^{-7}	0.026	0.589	0.029	0.027	0.009	0.221	0.066	0.063

collisions are not in phase with each other. Nevertheless, both quantities exactly balance each other on the average and both go to zero as $\omega/\nu_m^e \to \infty$.

Finally, it should be emphasized that one source of inaccuracy in these calculations is the neglect of the time dependences of the electron number density and of the vibrational distribution functions of molecules in the electronic ground states $N_2(X\ ^1\Sigma_g^+)$ and $H_2(X\ ^1\Sigma_g^+)$. However, the characteristic relaxation frequencies of these quantities are largely smaller than the values for the angular field frequency considered in this work, so that both the electron and the vibrational densities can be assumed here to be time independent. This would not be valid for the extremely low values of ω, but in this case the electrons follow the rf field instantaneously and, then, the electron transport can be very satisfactorily described using the Boltzmann equation for a dc field at the different time-varying values of the rf field strength.

ACKNOWLEDGMENTS

The author is indebted to Professor C. M. Ferreira and Professor R. Winkler for fruitful discussions.

[1] R. A. Gottscho, R. H. Burton, D. L. Flamm, V. M. Donnelly, and G. P. Davis, J. Appl. Phys. **55**, 2707 (1984); D. L. Flamm and V. M. Donnelly, *ibid.* **59**, 1052 (1986).

[2] R. Winkler, H. Deutsch, J. Wilhelm, and Ch. Wilke, Beitr. Plasmaphys. **24**, 303 (1984); R. Winkler, J. Wilhelm, and A. Hess, Ann. Phys. (Leipzig) **42**, 537 (1985); R. Winkler, M. Capitelli, M. Dilonardo, C. Gorse, and J. Wilhelm, Plasma Chem. Plasma Processing **6**, 437 (1986); R. Winkler, M. Dilonardo, M. Capitelli, and J. Wilhelm, *ibid.* **7**, 125 (1987).

[3] T. Makabe and N. Goto, J. Phys. D **21**, 887 (1988); N. Goto and T. Makabe, *ibid.* **23**, 686 (1990).

[4] G. L. Rogoff, J. M. Kramer, and R. B. Piejak, IEEE Trans. Plasma Sci. **PS-14**, 103 (1986); R. J. Seeböck and W. E. Köhler, J. Appl. Phys. **64**, 3855 (1988).

[5] T. Holstein, Phys. Rev. **70**, 367 (1946); S. C. Brown, in *Gas Discharges II,* edited by S. Flügge, Handbüch der Physik Vol. 22 (Springer, Berlin, 1956), p. 531.

[6] C. M. Ferreira and J. Loureiro, J. Phys. D **17**, 1175 (1984); **22**, 76 (1989).

[7] M. Capitelli, R. Celiberto, C. Gorse, R. Winkler, and J. Wilhelm, J. Phys. D **21**, 691 (1988).

[8] W. E. Köhler, R. J. Seeböck, and F. Rebentrost, J. Phys. D **24**, 252 (1991).

[9] H. Margenau and L. M. Hartman, Phys. Rev. **73**, 309 (1948).

[10] L. C. Pitchford and A. V. Phelps, Phys. Rev. A **25**, 540 (1982).

[11] A. V. Phelps and L. C. Pitchford, Phys. Rev. A **31**, 2932 (1985).

[12] W. P. Allis, in *Electron-Emission. Gas Discharges I,* edited by S. Flügge, Handbüch der Physik Vol. 21 (Springer, Berlin, 1956), p. 383.

[13] S. D. Rockwood, Phys. Rev. A **8**, 2348 (1973).

[14] L. S. Frost and A. V. Phelps, Phys. Rev. **127**, 1621 (1962).

[15] C. E. Treanor, J. W. Rich, and R. G. Rehm, J. Chem. Phys. **48**, 1798 (1968); B. F. Gordiets, Sh. S. Mamedov, and L. A. Shelepin, Zh. Eksp. Teor. Fiz. **40**, 1287 (1974) [Sov. Phys. JETP **40**, 640 (1975)].

[16] J. Loureiro and C. M. Ferreira, J. Phys. D **19**, 17 (1986).

[17] J. Loureiro and C. M. Ferreira, J. Phys. D **22**, 1680 (1989).

[18] E. Gerjuoy and S. Stein, Phys. Rev. **97**, 1671 (1955).